Calculating the Uncertainty of a
Structure from Motion (SfM) Model, Cadman Quarry, Monroe, Washington

Tait S Russell

Abstract

Structure from Motion (SfM) is a new form of photogrammetry that automates the rendering of georeferenced 3D models of objects using digital photographs and independently surveyed Ground Control Points (GCPs). This project seeks to quantify the error found in Digital Elevation Models (DEMs) produced using SfM. I modeled a rockslide found at the Cadman Quarry (Monroe, Washington) because the surface is vegetation-free, which is ideal for SfM and Terrestrial LiDAR Scanner (TLS) surveys. By using SfM, TLS, and GPS positioning at the same time, I attempted to find the deviation in the SfM model from the TLS model and GPS points. Using the deviation, I found the Root-Mean-Square Error (RMSE) between the SfM DEM and GPS positions. The RMSE of the SfM model when compared to surveyed GPS points is 17cm. I propagated the uncertainty of the GPS points with the RMSE of the SfM model to find the uncertainty of the SfM model compared to the NAD 1984 datum. The uncertainty of the SfM model compared to the NAD 1984 is 27cm. This study did not produce a model from the TLS that had sufficient resolution on horizontal surfaces to compare to surveyed GPS points.

Table of Contents

List of Figures

List of Tables

1.0 Introduction

Geospatial data is needed for military, scientific, and industry uses. Remote sensing is a major method of acquiring geospatial data. It is able to provide continuous-coverage geospatial data more easily and cheaply than in-person field methods that provide sparse point data. Geologic hazard mitigation relies greatly on precise and accurate geospatial data. For example, Digital Elevation Models (DEMs) can be used to model retreating bluffs, slope failures, and other forms of land movement that can be hazardous.

Structure from Motion (SfM) is a new and relatively inexpensive form of remote sensing. It is able to produce DEMs with cm-scale resolution for a small fraction of the cost of Light Detection and Ranging (LiDAR). Developing a more inexpensive form of remote sensing will allow for more geospatial data collection. However, because the technique is relatively new, there are only a few published studies that address the accuracy of landform models produced with SfM.

My project seeks to quantify the error found in DEMs derived from SfM methodology. I modeled a rockslide found at the Cadman Quarry (Monroe, Washington) because the surface was vegetation-free, which is ideal for SfM and TLS (Terrestrial LiDAR Scanner) surveys. See Figure 1, Figure 2, and Figure 3 for the site location. By using SfM, TLS, and GPS positioning at the same time, I attempted to find the deviation in the SfM model from the TLS model and GPS points. I then propagated the deviation with the accuracy of the GPS points to find the uncertainty of the SfM model.

2.0 Background

2.1 Prior Work

Unmanned Aerial Vehicles (UAVs) with digital cameras can map landslides quickly and with high precision (Niethammer et al., 2012). UAVs are also known as sUAVs (small Unmanned Aerial Vehicles), UASs (Unmanned Aerial Systems), sUASs (small Unmanned Aerial Systems), or simply "drones". According to Neithammer et al. (2012), photogrammetry experiments using UAV platforms were started by Prybilla and Wester-Ebbinghaus in 1979. Also according to Neithammer et al. (2012), the first high-resolution Digital Terrain Model (DTM) using autonomous UAVs was created by Eisenbeiss et al. in 2005.

Niethammer et al. (2012) surveyed the Super-Sauze landslide using UAVs. They created an orthographic image with 4cm resolution and Digital Terrain Models (DTMs) with between 3cm and 8cm resolution (depending on flight heights between 100m and 250m) (Niethammer et al., 2012). The UAV-photogrammetry-derived DTM, when compared to their TLS scan, had a Root-

Mean-Square Error (RMSE) of 31cm in the vertical direction (Niethammer et al., 2012). When compared to their GCPs (Ground Control Points), the errors were 7.9cm in the x-direction, 7.9cm in the y-direction, and 18.5cm in the vertical direction (Niethammer et al., 2012). The errors are considered high and are due to the vegetation obscuring the ground surface (Niethammer et al., 2012).

Other studies have shown some statistical information regarding the resolution and accuracy of UAV-photogrammetry-derived DTMs. Chander et al. (2002) created a DTM with 20cm resolution and a RMSE of 4.5cm (Chander et al., 2002). Levine et al. (2014) created DTMs with resolutions between 5cm and 10cm, but no accuracy information was available in the published abstract (Levine et al., 2014). Westboy et al. (2012) found that 100% of the UAV-photogrammetry-derived DTM cells differ from a TLS scan within +/-50cm on a non-vegetated surface, but no RMSE was reported. Russell et al. (2014) created a DTM of a glacier terminus with 7cm resolution and a RMSE of 40cm (estimated using Agisoft PhotoScan Pro software after construction of the DTM).

In 2012, Dr. Andrew Ritchie developed an airplane-mounted camera system to collect aerial imagery of the Elwha River and Elwha Delta (Andrew Ritchie, National Parks Service, written communication, 2015). He uses the photographs to develop SfM models of the Elwha with an accuracy of +/-20cm relative to LiDAR scans (Andrew Ritchie, National Parks Service, written communication, 2015). Using the models, Dr. Ritchie can calculate sediment erosion and deposition in near-real time (Andrew Ritchie, National Parks Service, written communication, 2015). Since he began in 2012, he has run about 80 SfM flights over the Elwha (Andrew Ritchie, National Parks Service, written communication, 2015).

The work of Lane et al. (2000) and Micheletti et al. (2015) provides useful information on gathering photographs using UAVs for the purpose of photogrammetry. Lane et al. (2000) found that UAV-photogrammetry-derived DTM accuracy is limited by image scale and scanning density. Micheletti et al. (2015) provides a list of important factors to consider when acquiring the photographs:

- It is better to collect images from multiple altitudes.
- Photographing the whole site in a few images, then moving in closer for detail is best.
- Using a flash can change the lighting conditions, which makes it harder for SfM software to reconstruct the area, so no flash is best.
- Consistent lighting is best.
- It is also best to collect photographs from as many positions as possible.
- The more images, the more precise and accurate the model will be.
- The survey area should also be static.

- There will be issues in areas that have high transmissivity, high reflectivity, and/or are highly homogenous.

2.2 Study Site

Cadman Quarry is located along Highway 203 about 3 miles south of Monroe, WA. The location of the quarry was over-run by the Cordilleran Ice Sheet during the last glaciation. The related fluvial-glacial rivers deposited sands and gravels, which are mined for construction purposes. Also, the quarry is within a fault system (Troost, 2015). The fault system brought bedrock near the surface, which is rarely found near the surface in the Puget Lowlands. The ability to quarry hard-rock, sands, and gravels within the same site is why Cadman is excavating the area.

Along the east benches of Cadman Quarry, there is a rockslide in one of the hard-rock quarry bench roads. The rock has fractured nearly vertically, sliding down and away from the scarp, leaving a large tension crack about 10 meters wide between the rockslide and the scarp. The rockslide did not have any movement in 2015 (Robby Johnson, Cadman Inc., oral communication, 2015).

The rockslide at Cadman Quarry was chosen for this study because it is unvegetated. Vegetation obscures the ground in photographs, resulting in poorer ground coverage and a lower quality SfM model.

3.0 Methods

3.1 Making GCP Targets

Before conducting the survey, I made thirty Ground Control Point (GCP) targets for both georeferencing the SfM model and for error checking. See Figure 4. Each target was made by cutting a square approximately 35cm by 35cm out of a light-blue tarp. I then placed a small, square piece of orange tape (approximately 4cm by 4cm) in the center of the target to be the "bullseye" where the GPS measurement was taken. The bright orange is intended to be easily seen in the collected photographs. In order to differentiate the GCP targets, I taped a large number on each target using orange tape. I also taped a single stretch of orange tape beneath the number for orientation (differentiating numbers like "12" and "21").

3.2 Placing and Measuring GCP Targets

The survey was on done January 2nd, 2016. We started at about 11:00am (PST). It was a clear, sunny day with temperatures around 45 degrees Fahrenheit.

Once in the field, I placed the GCP targets and measured their GPS location. The original plan was to place GCP targets east, west, north, and south of the sliding bench. However, the bench east the slide was marked as "do not enter", so the GCP targets were placed on the next bench east. Unfortunately, the south side of the bench was completely inaccessible. A total of seventeen targets were placed around the sliding bench. See Figure 5. GCPs with identifier numbers less than 20 were placed for georeferencing the SfM model, whereas GCPs with identifiers 20 and greater were placed for error checking. I placed the modeling-GCPs along the sides of the benches to better constrain the edges of the benches, whereas I placed the error-checking-GCPs along the center of the benches to maximize the distance from the modeling-GCPs.

After placing each GCP target, I measured its GPS location using a Trimble Geo 7x with an external receiver. The Trimble Geo 7x is a GPS receiver/transmitter with a laser range finder. It is capable of marking GPS positions within 1cm horizontally and 1.5cm vertically when connected to a real-time base station (Trimble, 2015). I gathered GPS data with the external receiver until the estimated post-processing accuracy shown on the Trimble read 2cm. To keep track of which GPS measurement went with which GCP target, I saved the GCP target number in the comment section of each GPS measurement.

To increase the accuracy of the GCP data, the GPS points collected by the Trimble were run through GPS Pathfinder Office (v4.00) to apply differential processing corrections. Differential processing uses GPS information recorded at a stationary GPS base station to remove errors in the GPS measurements caused by fluctuations in the magnetosphere of the Earth. I used the following processing steps modified by instructions given by Brian Holmes (University of Washington: Earth and Space Sciences Department, written communication, 2014). For the differential processing in GPS Pathfinder Office, I used the "Automatic Carrier and Code Processing (Recommended)". I then selected "Use Multiple Base Providers" with default correction settings. I created a new base provider group and selected three base stations: a UNAVCO station in Issaquah, WA; a UNAVCO station in Bayview, WA; and a UNAVCO station in Darrington, WA. See Table 1. I selected these stations because they resulted in the best estimated accuracy reported by the program after trying every combination of on-line, rated base stations within 100km. After creating the base provider group, I had the program use the reference position from the base providers. Finally, I selected the "Sample ESRI Shapefile Set-Up" as the export (adding position attributes under "Properties").

After the GPS Pathfinder Office program finished processing and exporting the GPS points, I imported the point data into ArcMap (v.10.2.1.3497). Once imported, I defined the projection system because the shapefile did not have the projection system defined. I used the WGS 1984 coordinate system, which the Trimble was set to measure coordinates relative to. Finally, I exported the attribute table of the shapefile as a text file in order to import the GCPs into the SfM program, Agisoft PhotoScan Pro.

3.3 UAV SfM Survey

To collect the photographs needed for SfM, I flew a DJI Phantom 2 Vision+ (a civilian recreational drone). I used three DJI Phantom 2 Vision+ rechargeable batteries, with each allowing for about 15 minutes of flight (a total of about 45 minutes). The drone is equipped with a 14MP gimbal-stabilized camera.

The Phantom 2 Vision+ is not water resistant at all and cannot be used in wet conditions like rain, snow, or heavy fog (DJI, 2015). The drone also cannot fly in heavy winds nor under zero degrees Celsius (DJI, 2015). So, planning a survey date is weather-dependent. Luckily, the weather was a clear, sunny day with little to no wind during our survey of the quarry.

Because SfM works by using photographs, there must be enough ambient light to capture high-quality images. The ambient lighting conditions must be unchanging, otherwise SfM programs cannot find the patterns found between images needed to reconstruct the survey area. The drone SfM survey took about an hour, so the elevation of the sun changed by several degrees, slightly changing the shadow lengths and lighting conditions.

Because this study used a drone to acquire the images, Federal Aviation Administration (FAA) regulations had to be considered. When this survey was conducted on January 2nd, 2016, I flew under the FAA hobby aircraft guidelines. Along with not being able to use data for profit, this meant that I had to fly under the following rules (FAA, 2015):

- Fly below 400 feet and remain clear of surrounding obstacles.
- Keep the aircraft within visual line of sight at all times.
- Remain well clear of and do not interfere with manned aircraft operations.
- Don't fly within 5 miles of an airport unless you contact the airport and control tower before flying.
- Don't fly near people or stadiums.
- Don't fly an aircraft that weighs more than 55 lbs.
- Don't be careless or reckless with your unmanned aircraft – you could be fined for endangering people or other aircraft.

I was able to complete the survey without violating the FAA guidelines. Following the guidelines did not impede the aerial survey in any way.

Prior to flying the drone, I set the camera to automatically adjust its exposure, shutter speed, and aperture. I also set the camera to take a photograph every 3 seconds (as fast as it can). This procedure required photos to be captured in JPEG format, because RAW files (which are typically recommended for SfM) can capture only as fast as one photograph every 30 seconds.

For the first 30 minutes of flight-time, I collected low-altitude photographs of the bench faces. I did this by pointing the camera on the drone straight down and flying 5-15m above each bench. For best coverage, I flew in a "lawnmower" pattern. See Figure 6. To increase overlap between subsequent photographs and to reduce motion blur, I flew very slowly (0.5-1m/s). The amount of overlap between photographs was unknown during the survey.

For the last 15 minutes of flight-time, I collected high-altitude photographs of the bench faces as well as photographs of the rock walls. The high-altitude photographs were collected because Micheletti et al. (2015) recommends acquiring photographs from multiple altitudes. For the high-altitude photographs, the camera was kept pointed straight down while I flew at a height of about 25m. I flew across the survey area and back once at speeds less than 1m/s. Lastly, I collected photographs of the rock walls in the survey area. To do this, I set the camera on the drone to point forward while I flew slowly (0.5-1m/s) along each wall. I flew at a height about halfway up each wall, and back away from the wall far enough for the vertical extent of each wall to be captured in each photograph.

3.4 TLS Survey

A Riegl VZ-4000 Terrestrial LiDAR System (TLS) was used to collect the LiDAR data. The TLS is capable of scanning from up to 4km away with an angular resolution as small as 0.0005 degrees, and a precision of 1cm at 150m (Riegl, 2015). So, the TLS can be used for very high-resolution modeling.

Three locations were selected from which to scan the quarry with TLS: one north of the sliding bench, one south of the slide, and one west of the slide. The locations were selected because they were the highest elevations locations from which to scan the rockslide with the TLS. The three scan locations are shown in Figure 7.

At each scanning location, we placed four of the TLS reflector targets around the TLS, 5-15m away at slightly different elevations, to enable the TLS system to correctly orient and georeference itself. For each of the three scans, we set the TLS to do a 360 degree panorama scan at 50kHz with an angular resolution of 0.08 degrees. We also set the TLS to collect photographs for each scan, which allows for colorization of the TLS model. By draping the

6

photographs collected by the TLS over the point cloud model, the survey area can have a colorized texture, which is needed to locate the GCPs.

3.5 Post-Processing Aerial Photographs

The GPS information stored as geotags in the photographs collected by the drone is not of sufficient accuracy to use in SfM. When loaded into Agisoft PhotoScan Pro, the photographs were grouped together in a perfect grid pattern, which indicates the GPS information in the geotags is not accurate. The altitudes were all recorded as 0m because the DJI Phantom 2 Vision+ does not store altitude information in the geotags. If the geotags were used, Agisoft PhotoScan Pro would have trouble properly aligning the photographs when the geotags indicate a false position.

These geotags must be removed from the metadata for each photo; otherwise, the SfM software (Agisoft PhotoScan Pro) may incorrectly place and align the camera positions. To quickly and easily remove the GPS data from all of the photographs at once, I used an open-source script program called "EXIFtool" (Harvey, 2016). Using the command "exiftool -gps:all= - xmp:geotag= DJI*.jpg", I was able to remove the geotags from all of the photographs collected by the drone (Ask Ubuntu, 2013).

3.6 Creating SfM Model

The computer I used to run the SfM software was a Dell Precision Tower 7000 Series. It uses two Intel Xeon hyper-threading 6-core processors (a total of 12 cores that simulate 24 by hyper-threading). The computer is also equipped with two graphics cards: a GeForce GTX 780 Ti and a Quadro 4000. The computer has 64GB of RAM.

The program I used for SfM modeling on this project was Agisoft PhotoScan Pro (v.1.2.3). I started by creating a new project and loading the post-processed photographs. Next, I created the sparse point cloud by aligning the photographs using the "high" accuracy setting for the greatest accuracy. The sparse cloud is a point cloud of the features/patterns found between the aligned photographs. For the sparse cloud alignment, I set the photograph selection to "generic" because the photographs no longer have geotags (Agisoft, 2016). Also, I increased the maximum number of points (features/patterns detected by Agisoft PhotoScan Pro in each photograph) to 400,000 and the maximum number of ties (corresponding features/patterns detected in other photographs) to 10,000. I did this because the console processing report showed that the program was finding more points than the default maximums of 40,000 points and 1,000 ties. After the sparse cloud was created, I deleted the extraneous points that were generated outside the survey area to reduce the processing time of generating the dense point cloud.

Next, I imported the GCPs as the markers into the program using the attribute table exported from ArcMap. I then found and placed the GCP marker on the target bullseye of each GCP target placed for georeferencing (GCP identifiers less than 20) in three photographs. That allowed the program to estimate the placement of the GCP markers in the rest of the photographs. I then adjusted and placed the markers. Markers were not placed in photographs that were taken at high-altitude or where the GCP is visible only along the periphery of the photograph. After placing the GCPs meant for georeferencing the model, I had the program optimize the estimated camera lens distortion. With these settings in place, I updated the photograph alignments, estimated camera positions, and sparse cloud.

After finishing the sparse point cloud, I generated a dense point cloud. The dense point cloud is a denser point cloud created based on the estimated camera positions (Agisoft, 2016). The program calculates depth information for each photograph to create the dense point cloud (Agisoft, 2016). I set the cloud density to "medium" because higher settings can over-interpolate and create noisy surfaces (David Shean, University of Washington: Earth and Space Sciences Department, oral communication, 2014). Also, I set the depth filtering to "mild" because there was no vegetation and the survey area was full of angular, jagged surfaces that I do not want to have smoothed out. Once the dense point cloud was generated, I deleted poorly modeled points generated in the periphery of the survey area.

With the model finished, I built a DEM using the dense point cloud. I then exported a georeferenced TIFF file for the DEM using the WGS 1984 State Plane Washington Zone 10N (meters) coordinate system because it is easier to measure the error in ArcMap using meters than it is using degrees. I used the default pixel size of about 4.0cm suggested by the program. I also had the program estimate the bounding area, which writes the bounding latitude and longitude information into the metadata. See Figure 8.

Next, I generated an orthophoto based on the DEM surface and using the "average" texture setting. See Figure 5. Like the DEM, I chose to export the orthophoto as a georeferenced TIFF file using the WGS 1984 State Plane Washington Zone 10N (meters) coordinate system. Again, I used the default pixel size suggested by the program (about 1.0cm) and allowed the program to estimate the bounding area.

3.7 Processing TLS Data

First, I opened the project file saved during the survey in RiScan Pro (v.2.0.3). Next, I loaded the point cloud of each scan separately. I then found objects in the survey area that could be used as tie-points between the three scans. See Figure 9. Using seven tie-points, the program was able to coregister the three scans. With the three scans coregistered, I converted the point cloud into an object. Finally, I created a mesh surface using the object. The mesh was generated using an

oblique view (about 270 degrees azimuth and 45 degrees elevation) because the mesh generates relative to the viewing angle, and the mesh was required on both the bench faces and walls.

3.8 Measuring SfM RMSE

The RMSE is a widely used single-value aspatial statistic indicating the deviation of estimated values within a data set from their true values (Erdogan, 2009). By squaring the difference between a data point and its true value, more weight is given to larger deviations. It has been used for many geospatial studies including landslides and remote sensing methodology comparisons (Erdogan, 2009; Hofierka et al., 2013; Sharma et al., 2010; Tan et al., 2014; Travelletti et al., 2012; Yao et al., 2014).

In ArcMap, I loaded in the GCPs defined by GPS data, the SfM orthophoto, and the SfM DEM. Using the measurement tool in ArcMap, I measured the horizontal difference between the GCPs and their corresponding target generated in the SfM orthophoto. To measure the elevation difference, I sampled the elevation value in the DEM cell where the corresponding GCP target was generated. I calculated the total offset between the Trimble-measured GCPs and the SfM-generated GCPs using Equation 1. I then calculated the RMSE using Equation 2.

Equation 1: $d = (h^2 + e^2)^{0.5}$
d is total offset distance.
h is horizontal offset.
e is elevation difference.

Equation 2: $RMSE = \sqrt[2]{\frac{\sum_{i=0}^{n} d_i^2}{n}}$
RMSE is the root-mean-square error.
d_i is the total offset of each GCP.
n is the number of GCPs used.

To know the uncertainty of the SfM model compared to the NAD 1984 datum, I propagated the uncertainty of the GCP measurements with the RMSE of the SfM model using Equation 3 (Shilpakar et al., 2016).

Equation 3: $u = (RMSE^2 + h^2 + v^2)^{0.5}$
u is the uncertainty of the SfM model.
RMSE is the root-mean-square error.
h is the horizontal accuracy of the GCPs.
v is the vertical accuracy of the GCPs.

9

3.9 Measuring TLS RMSE

Despite scanning from the highest elevation areas we could reach with the TLS, the survey did not collect enough points on the bench surfaces for a continuous mesh to be generated. Also, we were not able to collect any points in the tension crack at the head of the rockslide. This made it impossible to measure the TLS error using the GCPs placed on the benches.

4.0 Results

4.1 Trimble GCPs

A total of seventeen GCPs were collected in the survey area. Eleven of the GCPs were placed for georeferencing the SfM model and six for error checking. The vertical and horizontal accuracy of the GCPs are within 15cm. See Table 2.

4.2 UAV SfM

A total of 786 aerial photographs were collected by the drone to generate the SfM model. Agisoft PhotoScan Pro reported all locations within the survey area had at least nine overlapping images. Agisoft PhotoScan Pro found 6.15×10^5 points for the sparse cloud within the survey area and 3.60×10^7 points for the dense cloud. With that data, the program produced a DEM with a resolution of 4.0cm and an orthophoto resolution of 1.0cm. It took about 24 hours of processing time to generate the model and export the results.

Using ArcMap, I found that the RMSE of the SfM model compared to the surveyed GCPs is 17cm. See Table 3. When combined with the accuracy of the GCPs, the uncertainty of the SfM model compared to the NAD 1984 datum is 27cm.

4.3 TLS

Three scans were done using the TLS. RiScan Pro reported that the standard deviation of the tie-points between the three scans was about 33cm, which is higher than the 10cm found when using reflectors (Coire McCabe, University of Washington: Earth and Space Sciences Department, oral communication, 2016). With the three scans, a total of 6.55×10^5 points were collected in the survey area. Very few points were collected on the bench faces and none in the tension crack of the slide due to the low elevation of the scan positions and highly oblique angle of scanning. Hence, modeling of the bench faces and the tension crack was not possible. See Figure 10 and Figure 11. With gaps on the benches, I could not calculate the RMSE using the surveyed GCPs.

5.0 Discussion

The initial goals of this study were to calculate the RMSE of a SfM model compared to both a TLS model and GPS positions. I collected seventeen GCPs using a Trimble Geo 7x (eleven for the SfM model and six for error-checking). The GCPs have an accuracy within 15cm both horizontally and vertically. Using a drone, I collected 786 aerial photographs that I used to create a SfM model of the survey area. The resulting SfM DEM and orthophoto have resolutions of 4.0cm and 1.0cm, respectively. When compared to the GCPs, the SfM model has a RMSE of 17cm. When compared to the NAD 1984 datum, the SfM model has an uncertainty of 27cm. A sufficient TLS model was not able to be generated due to occlusions of many of the benches and the tension crack.

5.1 Trimble GCPs

Accurate measurements for the GCPs by the Trimble were paramount for this project. The accuracy of the GCPs must be high in order to have an accurate model as well as correctly estimate the RMSE in the SfM model. For the Trimble to report a real-time estimated horizontal accuracy of 2 cm, the Trimble had to collect data at each GCP for several minutes (about two to five). Placing and measuring the GCPs ended up being the most time-consuming part of the survey. Unfortunately, the in-field estimate of a 2 cm error was optimistic. Even though the Trimble collected data at each GCP until the post-processing accuracy was estimated to be 2cm, the errors reported by GPS Pathfinder Office after post-processing were up to 15cm horizontally and vertically.

I believe the accuracy could be improved if better base stations are used for the differential processing. For this study, I used three UNAVCO base stations. However, Washington State has a very accurate base station network (the Washington State Reference Network) that can, in principle, be used for differential processing. However, differential data is not available for the day of the survey.

On the benches of the quarry, the rock walls blocked the GPS signals from satellites in the eastern portion of the sky. In the field, I noticed fewer satellites were being used by the Trimble for GCPs close to the rock walls. I also noticed that my own body could interfere with the GPS signals, dropping the number of satellites connected to the Trimble when I stood near the external receiver.

With a Trimble, the user must be physically able to reach a location to measure the GPS location. At the quarry, I was unable to place GCPs to the south of the sliding bench because there was no accessible path to that area, which left the south side of the model barren of GCPs. I was also unable to place GCPs on the bench directly east of the sliding bench. That area was not permitted

11

for entry due to the danger of another bench failure. Agisoft (2016) recommends complete coverage of the survey area with GCPs for the highest accuracy.

Finally, correctly placing the GCPs in the locations desired was difficult. The quarry roads had been changed between the desk review of the site and the survey. With the roads changed, I was unable to correctly place the GCPs along the entire length of the western bench.

5.2 UAV SfM

Because the SfM model required the GCPs for georeferencing, the accuracy of the GCPs affect the accuracy of the model. The accuracy of the GCPs was within 15cm horizontally and vertically, which was substantially larger than the attempted 2cm. With more accurate GCPs, the accuracy of the SfM model will improve.

The SfM model also relies on digital photographs in order to render the scenery. Low-quality photographs (blurred, over/under exposed, small sensor chip, low Megapixel, etc.) will degrade the model. Because the Phantom 2 Vision+ uses a rolling shutter, it is susceptible to blurring if the drone is moving quickly (Andrew Ritchie, National Parks Service, written communication, 2015). However, I flew at such slow speeds (less than 1m/s) that the rolling shutter should not have affected the image quality.

Another possible issue with SfM surveying is not knowing what resolution the model will end up having. It is difficult (if not impossible) to predict what resolution the model will have. This could lead to either under-developing the model (too low of a resolution) or over-developing the model (wasting processing time). With most of the processing time automated by Agisoft PhotoScan Pro, I favored trying to over-develop the model, so critical features that needed to be modeled were not lost.

5.3 TLS

What most affected the ability of the TLS to scan the survey area was the location from which it scanned the survey area. The TLS is not capable of aerial surveying, so every part of the survey area must be viewable from ground positions. This was the limiting factor for our survey of the quarry. Because of the danger of bench failure, we were not allowed to walk beyond the line of boulders that stretch along the benches. This prevented us from being able to scan the sliding bench face from the benches to the north, south, and east. We attempted to scan the bench faces by scanning from the highest locations accessible. However, we were neither able to collect enough points on the bench faces to generate a model, nor were we able to collect any points within the tension crack of the slide.

The tie-points used can also be a source of error. The tie-points are needed to coregister the scans, bringing them together into one model. Tie-points are created by identifying and marking objects within the scanning area. Because the scans were set to a lower resolution of 0.08 degrees, most of the objects that could be used for tie-points were only partially modeled. This made it difficult to correctly place the tie-point in the same location in each of the three scans. The standard deviation of the tie-points was calculated by RiScan Pro to be about 33cm, which is higher than the 10cm possible when using reflectors (Coire McCabe, University of Washington: Earth and Space Sciences Department, oral communication, 2016).

6.0 Conclusions

6.1 Trimble GPS

Using a Trimble Geo 7x, I collected seventeen GCPs (eleven for SfM modeling and six for error-checking). See Figure 5. No GCPs were placed on the bench south of the rockslide due to the inaccessibility of the southern bench. The GPS data was post-processed using differential correction. Three UNAVCO base-stations were used for the differential processing. See Table 1. The post-processed horizontal and vertical accuracy of the GPS data was estimated by GPS Pathfinder Office to be less than 15cm. See Table 2.

6.2 UAV SfM

Using a drone and SfM, the entire survey area was surveyed aerially. The SfM model created using the aerial photographs was free of occlusions (gaps). The model resulted in an extremely high-resolution DEM and orthophoto (4.0cm and 1.0cm, respectively). See Figure 5 and Figure 8. However, the RMSE found in the SfM products was calculated to be 17cm. See Table 3. The uncertainty is 27cm compared to the NAD 1984 datum. I believe the uncertainty of the SfM products are so large in comparison to their resolution because of the poor quality of the GCPs. Had I placed more GCPs and measured them more accurately, I believe the RMSE and uncertainty could be much smaller because Agisoft (2016) recommends complete coverage of the survey area with GCPs.

6.3 TLS

Due to the data gaps along the bench faces and within tension crack at the head of the slide, the RMSE of the TLS could not be found. Had we been able to scan from higher elevations, we may have been able to scan the bench faces. However, we still would not have been able to scan within the tension crack of the slide.

The most limiting factor for the TLS in this study is that it was constrained to scanning from the surface of the ground. The TLS cannot scan horizontal surfaces at elevations higher than itself.

This can be a problem when attempting to scan areas with horizontal surfaces and high relief, or when there is limited access to locations from which to scan the area.

A TLS would be useful for scanning areas with minimally complex geometry. The less complex the geometry of the survey area, the few scanning locations will need to be used to eliminate occlusions. The rockslide at Cadman Quarry was too angular and complex to scan from the ground alone – aerial LiDAR would be needed for complete coverage. Formations like landslide scarps, bluffs, and road cuts would be ideal for TLS surveys.

7.0 Recommendations

7.1 Trimble GCPs

Because the estimated post-processing accuracy displayed in-field by the Trimble Geo 7x is not accurate, I highly recommend allowing the Trimble to continue collecting GPS data at each location well after it shows the post-processing accuracy desired. I also recommend connecting the Trimble to a hot-spot internet connection, so that it can apply the differential correction in-field.

The targets that I used for this study worked, but they could be improved. In most of the photographs, it was difficult to determine where the bullseye was in each GCP. Using the same quality camera that is attached to the Phantom 2 Vision+, I would recommend using larger targets, each with a larger identification number and bullseye. Another option would be to use the coded targets that can be generated and printed from Agisoft PhotoScan Pro. With large enough coded targets and/or a good enough aerial camera, Agisoft PhotoScan Pro can automatically detect the GCPs. This would eliminate the need to manually find each GCP within several photographs.

While not always physically possible, it is best to place GCPs around the entire survey area. Agisoft (2016) recommends this for maximum accuracy of the SfM model.

7.2 UAV SfM

While the DJI Phantom 2 Vision+ is easy to use and ready out-of-the-box, I recommend using a drone with a better camera and, if possible, use one that is also waterproof. Even though I flew at heights less than 15m for the high-quality images, it was difficult to resolve the information on each GCP in many of the photographs. It would be better to use a camera with a larger sensor, higher Megapixels, uses a global shutter (instead of a rolling shutter), and is capable of using a RAW file type for continuous photographing (instead of JPEG). Unlike JPEG, RAW does not compress the image data. Compressed images can reduce the quality of SfM models. Furthermore, with a drone that is waterproof, it is possible to survey under wet conditions.

Finally, it would be beneficial to use a drone and camera mount that is capable of correctly geotagging the aerial photographs. While geotags may not improve the accuracy or resolution of the SfM model, they will reduce the processing time Agisoft PhotoScan Pro needs to align the photographs and create the sparse point cloud (Andrew Ritchie, National Parks Service, oral communication, 2016).

As mentioned earlier, the GCP accuracy could be improved by allowing the Trimble to continue collecting data after it shows the desired post-processing accuracy. Increasing the accuracy of the GCPs will increase the accuracy of the SfM model. Also, placing more GCPs, especially on the south side (where none were able to be placed during our survey), would increase the accuracy of the SfM model (Agisoft, 2016). However, I do not know how much the accuracy would increase by doing so.

The "lawnmower" flight pattern worked well. However, more flight time would be useful. With a fourth or fifth battery, more photographs could have been collected around the perimeter of the site, where fewer points were found for the sparse and dense point clouds.

I recommend using the same processing steps that I used in Agisoft PhotoScan Pro. I also recommend using the same exporting steps that I used.

7.3 TLS

I recommend carefully considering what surfaces need to be scanned, then estimate scanning locations that will be able to view those surfaces. Be sure to pick scanning positions that are high enough to view the surfaces. It may be possible to see the surface from the scanning position when in the field, but if the surface is highly oblique from that scanning position, very few points may be collected on that surface. I recommend doing a quick, low-resolution scan of the area first, checking the point cloud to see if enough points will be collected from that position. Once a good position has been determined, then scan using higher-resolution settings.

Instead of using scanned objects within the study area as tie-points, I recommend using the TLS reflector targets. By placing the reflector targets in the study area, they can be used as tie-points. Because the reflectors return brighter laser pulses than the ground, they are easy to find in RiScan Pro. This can reduce the standard deviation between tie-points.

8.0 References

Agisoft, 2016, Help: PhotoScan Pro (v1.2.3): a Structure from Motion modeling program.

Ask Ubuntu, 2013, How can you delete only GPS metadata from a jpeg file?:
http://askubuntu.com/questions/236455/how-can-you-delete-only-gps-metadata-from-a-jpeg-file (accessed January 2016).

Chandler, J.H., Ashmore, P., Paola, C., Gooch, M., Varkaris, F., 2002, Monitoring river-channel change using terrestrial oblique digital imagery and automated digital photogrammetry: Annals of the Associated of American Geographers, v. 92, no. 1, p. 631-644.

DJI, 2015, Phantom 2 Vision+ User Manual v.1.8 (English):
http://dl.djicdn.com/downloads/phantom_2_vision_plus/en/Phantom_2_Vision_Plus_User_Manual_v1.8_en.pdf.

Erdogan, S., 2009, A comparison of interpolation methods for producing digital elevation models at the field scale: Earth Surface Processes and Landforms, v. 34, no. 3, p. 366-376.

FAA, 2015, Model Aircraft Oporations: https://www.faa.gov/uas/model_aircraft/ (accessed January 2016).

Google Earth, 2016, Cadman Quarry, 47°48'56.74"N, 121°57'38.73"W, Landsat June 8th, 2015 (accessed January, 2016).

Google Earth, 2016, Monroe, 47°51'24.11"N, 121°58'04.91"W, Landsat April 9th, 2013 (accessed February, 2016).

Harvey, P., 2016, EXIFTool: a program that modifies the EXIF information within programs: http://www.sno.phy.queensu.ca/~phil/exiftool/.

Hofierka, J., Gallay, M., Kanuk, J., 2013, Spatial Interpolation of Airborne Laser Scanning Data with Variable Data Density: Proceedings of the 26th International Cartographic Conference.

Lane, S.N., James, T.D., Crowell, M.D., 2000, Application of digital photogrammetry to complex topography for geomorphological research: The Photogrammetric Record, v. 16, no. 1, p. 793-821.

Levine, N., Ali, K., Chadwick, J., 2014, LIDAR Verses drone: DEM creation, accuracy, and other issues: Geological Society of America Abstracts with Programs, v. 46, no. 6, p. 297.

Micheletti, N., Chandler, J.H., Lane, S.N., 2015, Structure from Motion (SfM) Photogrammetry: British Society for Geomorphology, Geomorphological Techniques, Ch. 2, Sec. 2.2, ISSN 2047-0371.

National Park Service (NPS), 2003, European and Euro-American History: Olympic National Park, http://www.nps.gov/olym/planyourvisit/upload/Euro-history_printer-friendly.pdf (accessed October 2015).

National Park Service (NPS), 2015, About US: http://www.nps.gov/aboutus/index.htm (accessed October 2015).

Niethammer, U., James, M.R., Rothmund, S., Travelletti, J., Joswig, W., 2012, UAV-based remote sensing of the Super Sauze landslide: evaluation and results: Engineering Geology, v. 128, no. 1, p. 2-11.

Riegl, 2015, Riegle VZ-4000: http://www.riegl.com/uploads/tx_pxpriegldownloads/DataSheet_VZ-4000_2015-03-24.pdf (accessed January 2016).

Russell, T., Shean, D., Crider, J., 2014, A high-resolution DEM timeseries to measure glacial mass balance, dynamics, and variability at Mount Baker, WA USA: Geological Society of America Abstracts with Programs, v. 46, no. 6, p. 105.

Sharma, A., Tiwari, K. N., and Bhadoria, P. B. S., 2010, Quality assessment of contour interpolated digital elevation models in a diverse topography: International Journal of Ecology & Development, v. 15, no. W10, p. 26-42.

Shilpakar, P., Oldow, J. S., Walker, J. D., Whipple, K. X., 2016, Assessment of the uncertainty budget and image resolution of terrestrial laser scans of geomorphic surfaces: Geosphere, v. 12, no. 1, p. 281-304.

Tan, Q., Xu, X., 2014, Comparative Analysis of Spatial Interpolation Methods: an Experimental Study: Sensors & Transducers, v. 165, no. 2, p. 155.

Travelletti, J. and Malet, J.P., 2012, Characterization of the 3D geometry of flow-like landslides: A methodology based on the integration of heterogeneous multi-source data: Engineering Geology, v. 128, no. 1, p. 30-48.

Trimble, 2015, Trimble Geo 7x Datasheet: http://trl.trimble.com/docushare/dsweb/Get/Document-730024/022516-098A_Geo%207Xw%20Access_DS_US_0415_LR.pdf (accessed February 2016).

Troost, K., 2015, Cadman Quarry: https://canvas.uw.edu/courses/947181/files (accessed February 2015).

Westoby, M., Brasington, J., Glasser, N., Hambrey, M., Reynolds, J., 2012, 'Structure-from-Motion' photogrammetry: A low-cost, effective tool for geoscience applications: Geomorphology, v. 179, no. 1, p. 300-314.

Yao, L, Huo, Z., Feng, S., Mao, X., Kang, S., Chen, J., Xu, J., Steenhuis, T.S., 2014, Evaluation of spatial interpolation methods for groundwater level in an arid inland oasis, northwest China: Environmental Earth Sciences, v. 71, no. 4, p. 1911-1924.
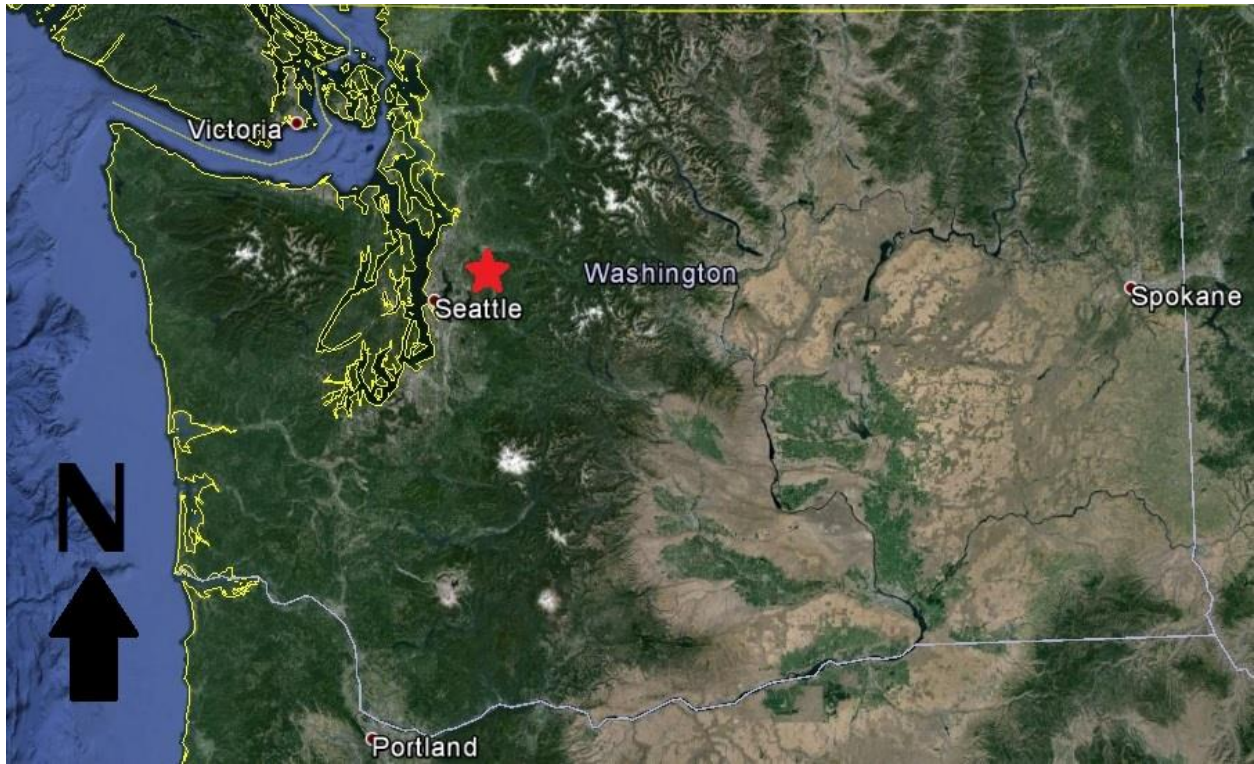
Figure 1: Aerial image showing the location of the Cadman Quarry site in Washington State (marked by the red star). (Google Earth a, 2016)

Figure 2: Aerial image showing the location of the Cadman Quarry site (marked by the red star). (Google Earth a, 2016)

Figure 3: Aerial image of Cadman Quarry (Google Earth b, 2016). The rockslide is shown within the orange circle.

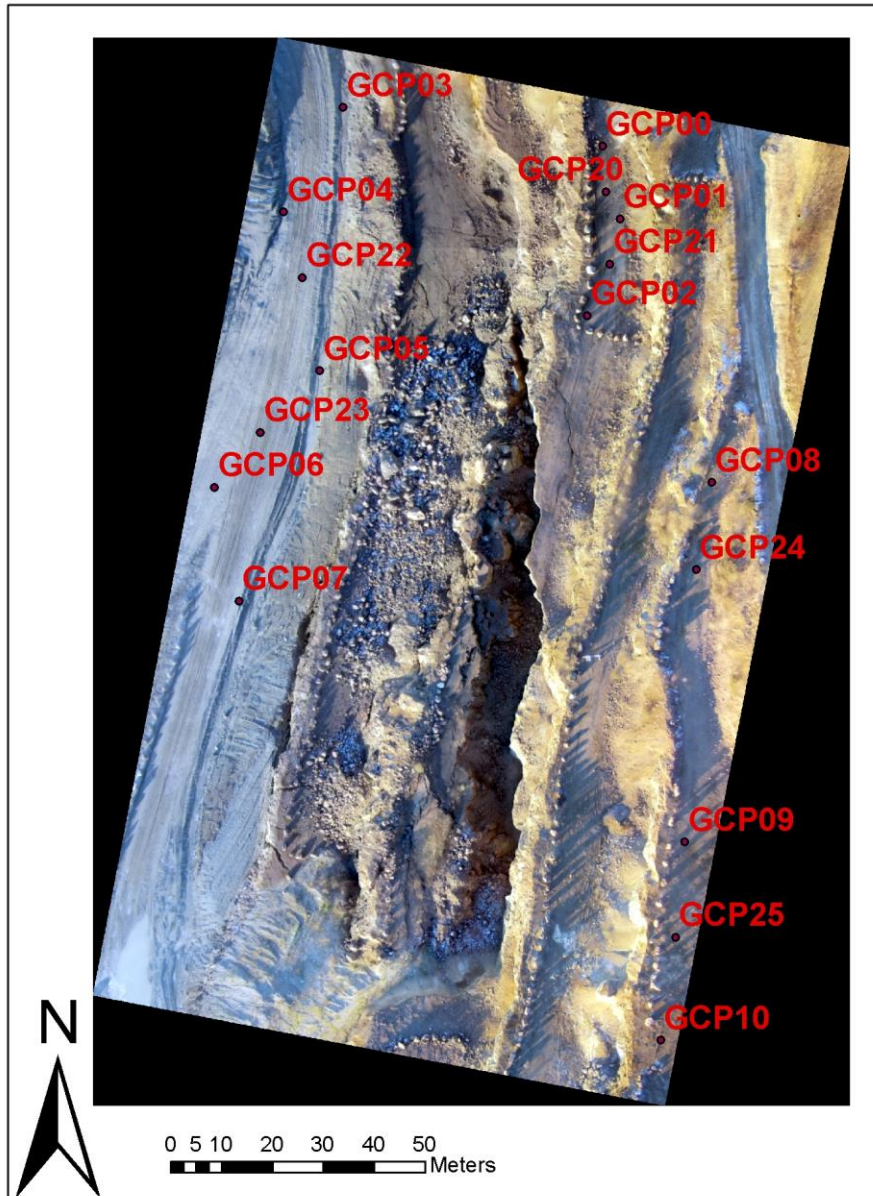Figure 4: Aerial photograph of GCP #0. The GCP is about 35cm by 35cm.

Figure 5: Composite orthophoto of Cadman Quarry derived from the SfM DEM, with GCP placement around the rockslide study area. A total of seventeen GCPs were placed. The rockslide and tension crack in the center were well resolved. The resolution is high enough that the safety boundary boulders around the bench perimeters are also well resolved. Resolution: 1.0cm.
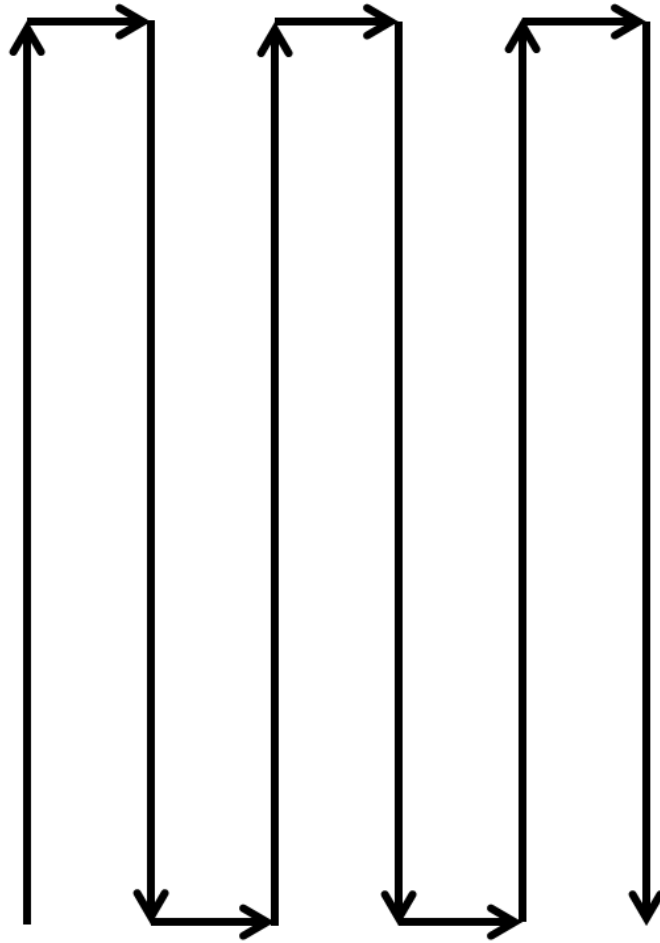
Figure 6: General "lawnmower" flight path used for this study.

Figure 7: Aerial photograph showing the TLS scanning locations using stars (Google Earth b, 2016). The scanning locations are represented by the green stars.
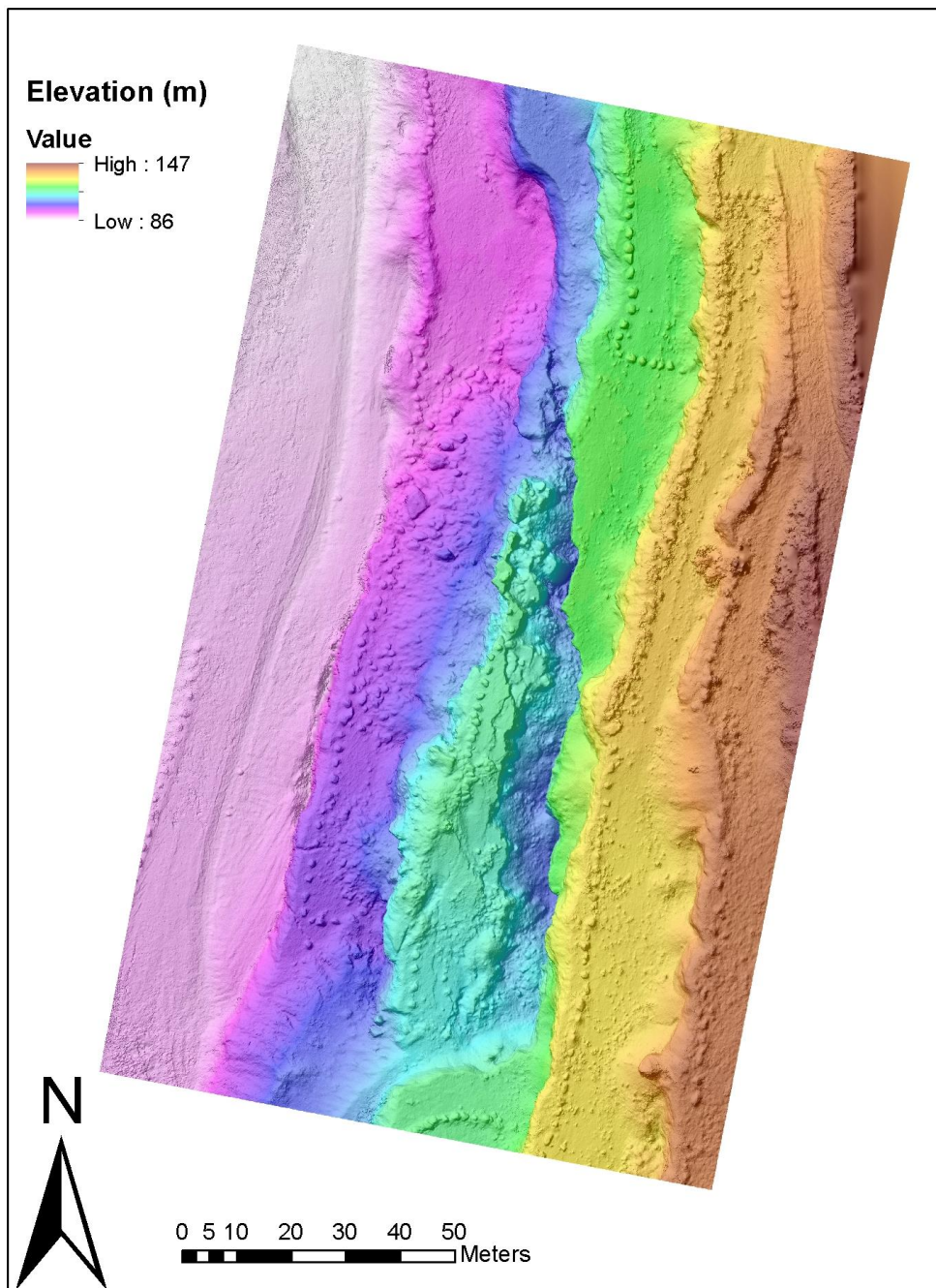
Figure 8: This is a DEM map over a hillshade of the rockslide at Cadman Quarry derived using SfM. The bench of the rockslide can be seen in blue-green near the center. Resolution: 4.0cm.
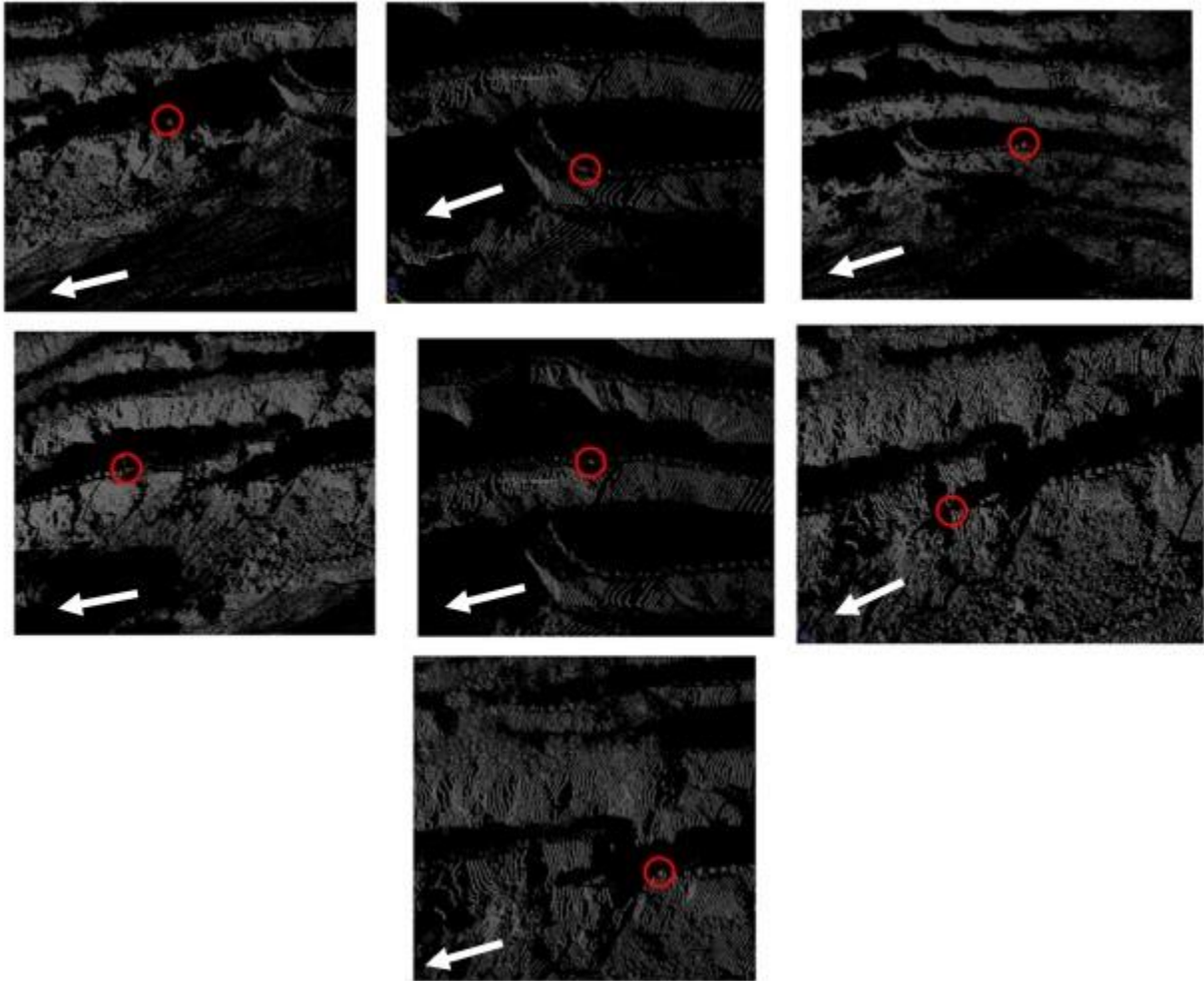
Figure 9: These images show each tie-point (represented by the red dot within the red circle) used to coregister the three TLS scans. The dark areas are the benches, whereas the white/grey areas are the rock walls. The white arrows point north.

Figure 10: Coregistered point cloud of the three TLS scans. The black areas are the benches, whereas the white/blue areas are the walls.
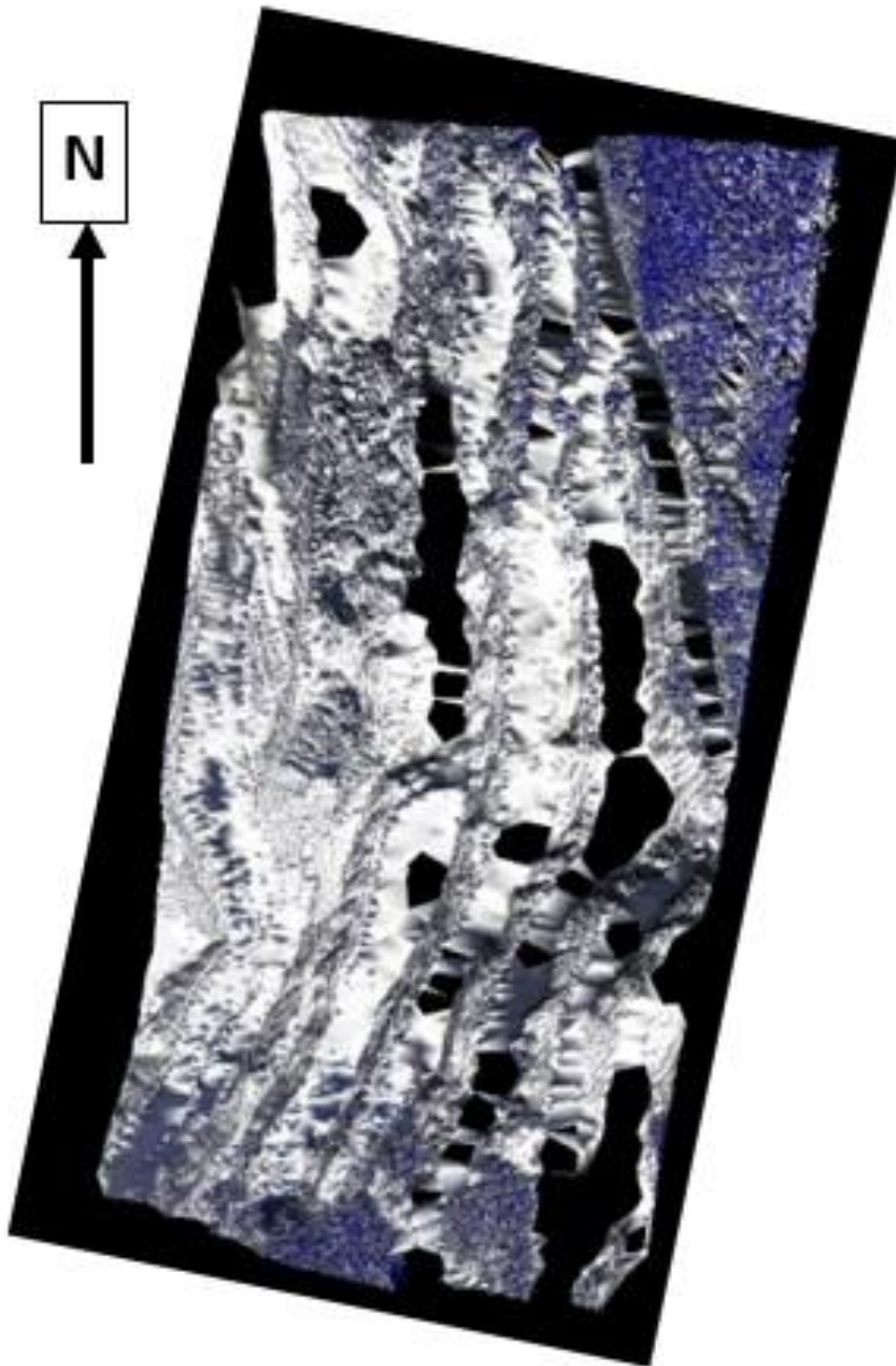
Figure 11: TLS mesh derived from the coregistered point cloud. The white/blue areas were modeled, whereas the occlusions are black.

Table 1: Base stations used for differential processing the GCP data. The integrity index is a 0 to 100 rating of the data quality from the station.

Provider	Location	Distance from Station to Site (km)	Integrity Index
UNAVCO	Issaquah, WA	36	78.03
UNAVCO	Bayview, WA	42	84.72
UNAVCO	Darrington, WA	55	73.75

Table 2: GCP data used for this study and their accuracy estimated by GPS Pathfinder Office. The coordinate system is WGS1984 (meters).

| GCP	Vertical Accuracy (m)	Horizontal Accuracy (m)	Elevation (m)	Latitude	Longitude
GCP00	< 0.15	< 0.15	120.369	47.81698622	-121.9601073
GCP01	< 0.15	< 0.15	120.091	47.81685712	-121.9600636
GCP02	< 0.15	< 0.15	120.238	47.81668651	-121.9601532
GCP03	< 0.15	< 0.05	87.454	47.81706087	-121.960786
GCP04	< 0.15	< 0.15	88.148	47.81687723	-121.9609461
GCP05	< 0.15	< 0.05	89.364	47.81659539	-121.9608566
GCP06	< 0.15	< 0.05	90.146	47.81639172	-121.9611371
GCP07	< 0.15	< 0.05	90.565	47.81618976	-121.9610777
GCP08	< 0.15	< 0.15	139.325	47.81638859	-121.9598321
GCP09	< 0.15	< 0.15	140.765	47.81575311	-121.9599157
GCP10	< 0.15	< 0.15	140.786	47.81540274	-121.9599864
GCP20	< 0.15	< 0.15	120.196	47.81690552	-121.9600997
GCP21	< 0.15	< 0.15	120.085	47.81677741	-121.9600918
GCP22	< 0.15	<0.05	88.937	47.81676082	-121.9608992
GCP23	< 0.15	< 0.05	90.001	47.81648793	-121.9610153
GCP24	< 0.15	< 0.15	139.14	47.81623436	-121.9598759
GCP25	< 0.15	< 0.15	141.079	47.81558434	-121.9599431

Table 3: RMSE calculations using the GCPs and SfM model.

GCP	GCP H Accuracy (m)	GCP V Accuracy (m)	(SfM-GCP) H Error (m)	GCP Elev (m)	SfM Elev (m)
20	< 0.015	< 0.015	0.025	120.196	120.127
21	< 0.015	< 0.015	0.053	120.085	119.941
22	< 0.05	< 0.015	0.067	88.937	89.031
23	< 0.05	< 0.015	0.04	90.001	90.001
24	< 0.15	< 0.015	0.08	139.14	139.296
25	< 0.15	< 0.015	0.194	141.079	140.852

(SfM-GCP) V Error (m)	(SfM-GCP) Error (m)	(SfM-GCP) Error^2
-0.069	0.0734	0.0054
-0.144	0.1534	0.0235
0.094	0.1154	0.0133
0	0.0400	0.0016
0.156	0.1753	0.0307
-0.227	0.2986	0.0892
	Average Error^2	0.0273
	RMSE (m)	0.17

Cadman Quarry SfM Hillshade
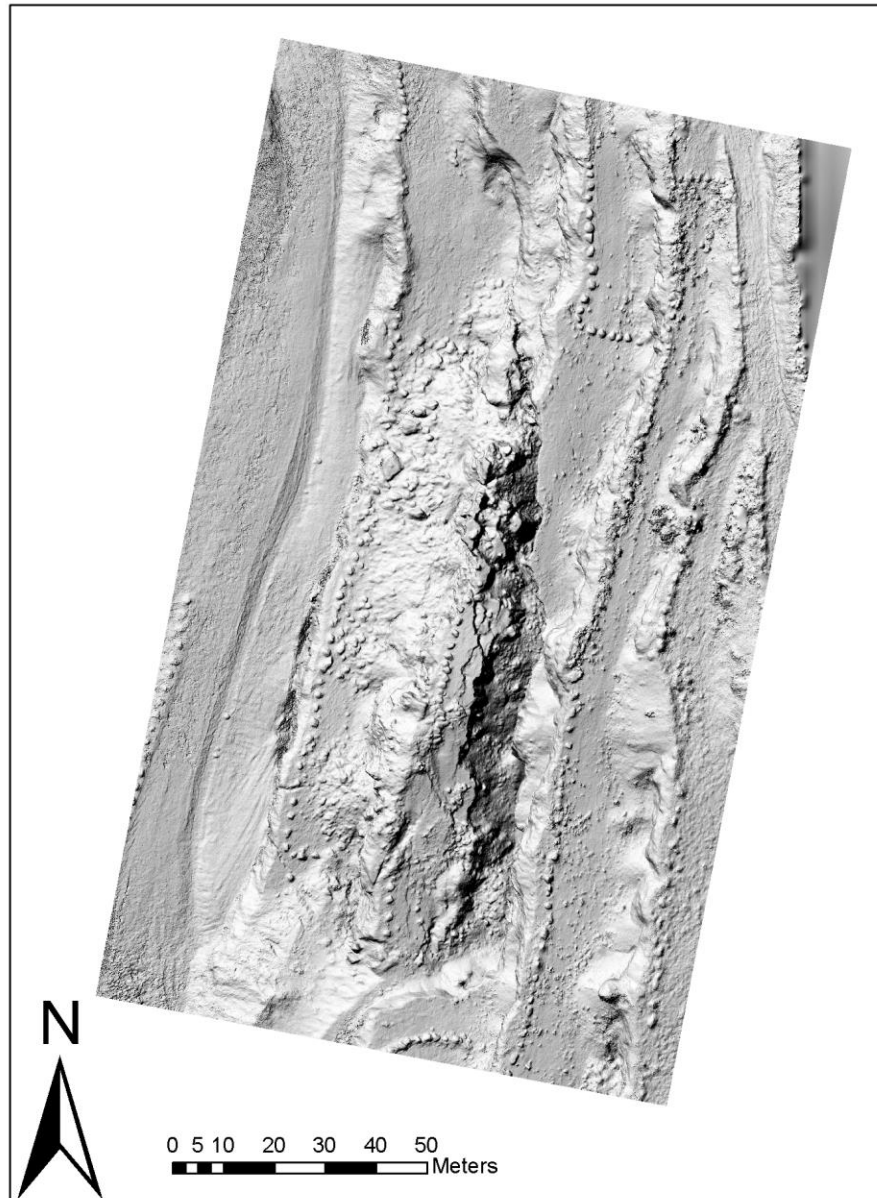
This is a hillshade of the rockslide at Cadman Quarry derived using SfM. Resolution: 4.0cm.

<u>Appendix B</u>

The purpose of the Master's in Earth and Space Sciences – Applied Geosciences (MESSAGe) internship project is to give students the ability to familiarize themselves with planning, implementing, and completing a research project with professionals in the geosciences industry. The MESSAGe internship project requires the students to each write a technical report covering their project as well as perform an oral presentation. Each student works under the guidance of a mentor who is skilled in the area of the student's research. Each student will also work with a group of two to three professional geoscientists, one of whom is the student's mentor, to review and edit the student's project proposal and technical report.